

DETERMINATION OF A TOPOGRAPHIC WETNESS INDEX USING HIGH RESOLUTION DIGITAL ELEVATION MODELS.

Majid HOJATI

Tehran University, Department of GIS and remote sensing, Tehran, Iran

majid.hojati@ut.ac.ir

Marzieh MOKARRAM

Shiraz University, Department of Range and Watershed, Agriculture College and Natural Resources of Darab, Shiraz, Iran

m.mokarram@shirazu.ac.ir

Abstract

Topographic wetness indices (TWIs) computed from digital elevation models (DEMs) are means to forecast the amount of moisture in the soil. In this study, using sub-pixel/pixel attraction the spatial resolution of digital elevation models (DEM) was increased. In the attraction, model scale factors of (2,3,4) with two neighboring methods of touching and quadrant are applied to DEMs in Matlab software for the study area. The algorithm is evaluated using 148 sample points that were measured by the researchers. As a result, it was shown that a spatial attraction model with a scale factor of (S=2) gives better results compared to the scale factors greater than 2 and also touching neighboring are more accurate than quadrant. The results showed that waterway obtaining from DEM with high spatial resolution is more accurate than DEM 90m. So according to the results, it is suggested that the same model for increasing spatial resolution of DEM in the studies must be used. Furthermore, the results of TWI map with the new DEM extracting of attraction model as input data showed that TWI has more details from the moisture of soil than the TWI map prepared with DEM 90m.

Keywords: Sup-pixel, Digital elevation model (DEM), Spatial resolution, Attraction models, topographic wetness index (TWI), GIS.

1. INTRODUCTION

Soil moisture is a key variable controlling hydrological and biogeochemical processes (Buchanan et al., 2014). Since its introduction, the TWI concept has been integrated into many popular hydrologic models (e.g., Schneiderman et al., 2007; SWAT-VSA, Easton et al., 2008) and pollution risk indices (Agnew et al., 2006; Sørensen et al., 2006; Reaney et al., 2011; Marjerison et al., 2011; Buchanan et al., 2013; Buchanan et al., 2014).

The accuracy of the TWI, as for any hydrological model, is depended on the surface topography. The existence of a DEM with high spatial resolution enables to the implementation of a detailed spatial hydrological model for an urban catchment. Therefore, a hydrologically sound DEM is needed to develop an appropriate TWI and delineation of a flood-prone (wet) area (Pourali et al., 2014).

Recently, advances in Geographic Information Systems (GIS) and an increase in the availability of high spatial resolution led to the increase of information about surface

topography, which is the primary data used to calculate a TWI. One of the important properties of DEM is a spatial resolution that represents the accuracy of DEM (Takagi, 1996). DEM as input data for the determination of TWI with variations in the spatial resolution can lead to different outputs. It can affect the attributes derived from them and influence models associated with them (Gallant and Hutchinson, 1997; Haile and Rientjes, 2005; Omer et al., 2003). There are many studies for the extraction of information of case study from different resolution DEM (Wolock and McCabe, 2000; Jenson, 1991; Hutchinson and Dowling, 1991, Mokarram and Sathyamoorthy, 2015). The results showed that this method can solve DEM associated problems efficiently and simulate flooding processes with a better accuracy. Buchanan et al. (2014) used different digital elevation model (DEM) resolutions for the determination of TWI. The results showed that fine-scale (3 m) LiDAR-derived DEMs worked better than USGS 10 m DEMs and, in general, including soil properties improves correlations

There are many methods for increasing the spatial resolution of DEM. For example, Shen et al. (2011) used Integration of the 2-D hydraulic model and high-resolution LiDAR-derived DEM for floodplain flow modeling. One of the models for increasing the spatial resolution is attraction model that is based on sub-pixel. Sub-pixel algorithm puts several classifications in the most plausible positions inside the pixel. This is made by assuming spatial dependence (Atkinson 1997). A linear optimization technique for sub-pixel mapping algorithm was created by Atkinson (1997) inspired of Verhoeye and De Wulf (2002).

The attraction model algorithm spatially depends on the neighborhoods of the central pixel which is attracting surrounding sub-pixels. Another possibility is the hypothesis of sub-pixel interaction as introduced by Mertens et al. (2003b) and Atkinson (2005). There are several methods for increasing sup-pixel by neighboring such as genetic algorithms (Mertens et al., 2003b) and pixel swapping (Atkinson, 2005) that use the initial pixel fraction values as a constraint.

This paper focuses on topographic wetness index (TWI) building with attraction model analysis of DEMs. In order to determine the TWI, the preparation of DEM with high resolution as input analysis is important. The generated TWI maps via DEM from attraction model and the primary DEM (Shuttle Radar Topography Mission (SRTM)) are compared. The methodology employed in this study is summarized in Figure 1.

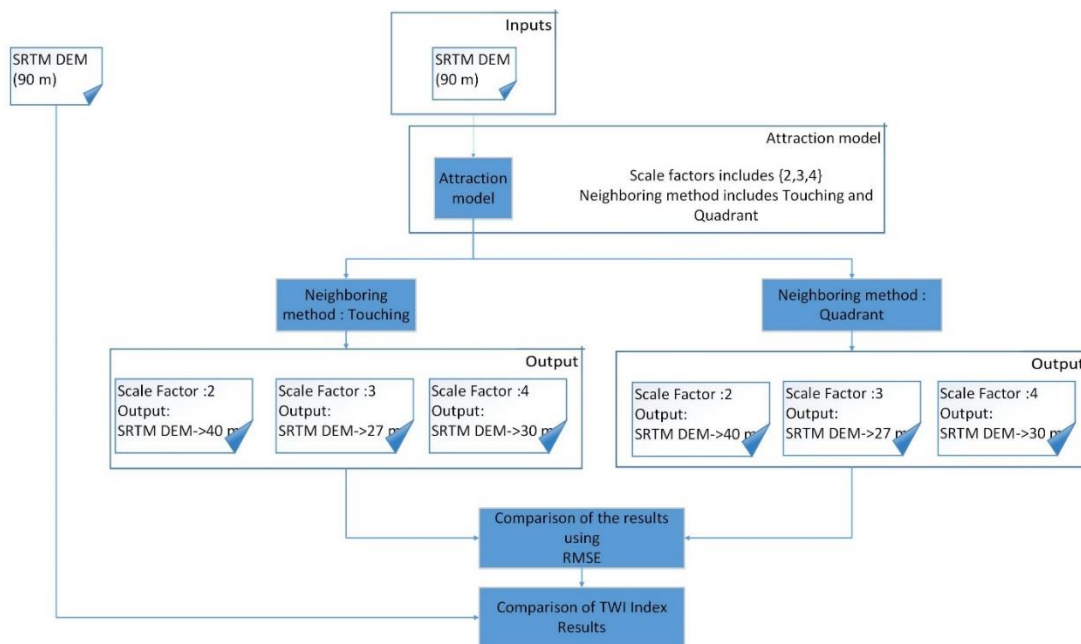


Figure 1: Flowchart for the methodology of TWI used in this study.

The steps of the flowchart in Figure 1 are as follow:

1. At the first step, the attraction model is run on SRTM DEM with a spatial resolution of 90m.
2. In attraction model both quadrant and touching methods and 3 scale factors of 2, 3 and 4 are tested for each neighboring method.
3. Then an RMSE index is calculated for each output of attraction model and the DEM with lowest RMSE is selected.
4. In the last step, the TWI model is applied on the original SRTM DEM and also the extracted DEM from attraction model and the result are compared.

2. MATERIALS AND METHODS

2.1. Data preparation

Shuttle Radar Topography Mission (SRTM) DEM data were downloaded from (<http://srtm.usgs.gov>) for free. We call it DEM 90m in this study. SRTM is one of the most comprehensive maps of elevation, NASA's Shuttle Radar Topography Mission (SRTM) (Werner, 2001; 48 Farr et al., 2007), covering mostly 80% of the Earth's surface, with a global resolution of 90 meters. The Shuttle Radar Topography Mission (SRTM) collected elevation data over 80% of earth's land area during an 11-day Space Shuttle mission. Ground station points were gathered from surveys done by National Cartographic Center of Iran (NCC). All needed preprocessing of points and DEMs were performed using ArcMAP version 10.3.

2.2. Attraction sub-pixel model

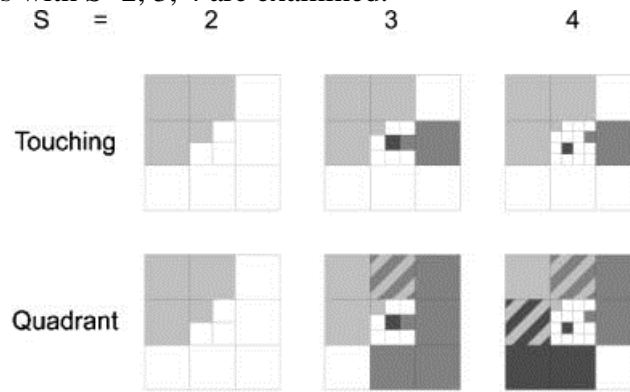
To obtain more details in a pixel, sub-pixel mapping was first introduced by Atkinson (Atkinson, 1997). Sub-pixel mapping is a technique designed to obtain the spatial distribution of different classes in mixed pixels at the sub-pixel scale by transforming fraction images into a classification map (XU et al., 2014). This is accomplished by assuming spatial dependence (Atkinson, 1997).

Attraction models are closely related to the field of geostatistics (Mertens, 2008). Sub-pixel mapping locates the different class fractions in the most plausible positions inside the pixel.

Sub-pixel methods are always used in satellite images but for the first time they were used for Digital elevation models. In this study, a sub-pixel spatial attraction model is used as a new method for increasing spatial resolution of digital elevation model (DEM). The sub-pixel attraction model is based on the fraction values in neighboring pixels acting towards sub-pixels inside a central pixel. The quadrant neighborhood and touching neighborhood are two different neighboring models which are used in attraction model. In the quadrant neighborhood a neighbor pixel is the only pixel in the same quadrant. While in touching neighborhood a neighbor pixel is the pixel which physically touches a sub-pixel. The illustration of two neighborhoods with different scale factors are shown in Figure 2 (Mertens et al., 2014).

A scale factor (S) shows the number of sub-pixels per pixel. According to Figure 2, all the pixels attracting a sub-pixel are explained in the same shade as the sub-pixel. For example, for the quadrant neighborhood and S=3 and touching method, the darkest shaded sub-pixel inside the center pixel is attracted only by the right middle pixel and the gray sub-pixel is attracted by the left top, top middle and left middle pixel. Shaded sub-pixels without corresponding pixels refer to the sub-pixels that are not attracted by any of the pixels, as is the case for the center

sub-pixels with $S=3$ for the touching and quadrant neighborhood. In this paper, two neighborhood methods with $S=2, 3, 4$ are examined.



Source: Mertens et al., 2014.

Figure 2: Graphic of sub-pixel attraction model for different neighborhoods and scale factors.

The neighborhoods previously defined (figure 2) can now be mathematically formulated as (Mertens et al., 2014):

N Touching neighborhood:

$$N_1[p_{a,b}] = \{p_{i,j} \mid d(p_{a,b}, p_{i,j}) \leq \frac{1}{\sqrt{2}}(S+1)\} \quad (1)$$

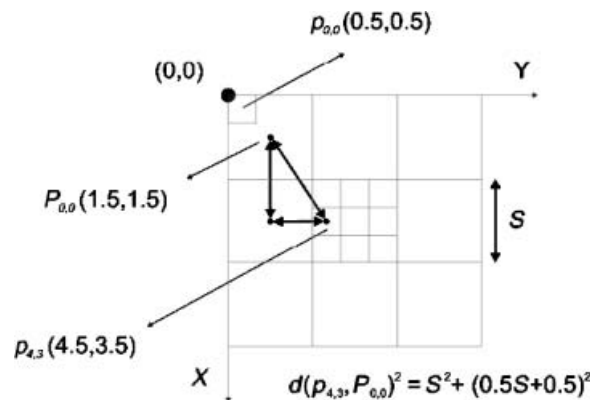
N Quadrant neighborhoods:

$$N_2[p_{a,b}] = \{p_{i,j} \mid d(p_{a,b}, p_{i,j}) \leq \frac{1}{\sqrt{2}}(2S-1)\} \quad (2)$$

With the distance defined as:

$$d(p_{a,b}, p_{i,j}) = \sqrt{[a+0.5-S(i+0.5)]^2 + [b+0.5-S(j+0.5)]^2} \quad (3)$$

The coordinate system which the distance for pixel and sub-pixels are calculated based on is shown in Figure 3 (Mertens et al., 2014):



Source: Mertens et al., 2014).

Figure 3: The coordinate system and the distance calculation between pixels and sub-pixels.

In fact, for different neighborhoods, attraction values can be computed for all sub-pixels inside a pixel. After choosing each pixel set for each sub-pixel the attraction value for each pixel is calculated using Eq.4.

$$p_{a;b} (c) = Avg\left\{\frac{P_{i;j}(c)}{d(p_{a;b}, P_{i;j})} \mid P_{i;j} \in N_t[p_{a;b}]\right\} \quad (4)$$

- $P_{a;b(c)}$ is the attraction value for sub-pixel $p_{a;b}$ and class c .
- $P_{i;j(c)}$ is the fraction value for pixel $P_{i;j}$ and class c .
- S is the scale factor
- $N_t[p_{a;b}]$ is the neighborhood of type t of sub-pixel $p_{a;b}$.
- $d(p_{a;b}, P_{i;j})$ is the distance for sub-pixel $p_{a;b}$ and pixel $P_{i;j}$.

After this stage, then raw attraction values can be computed. These values can then be used to attach the proper class to each sub-pixel: Classes with highest attractions are attached first.

2.3. Topographic Wetness Index (WTI)

The topographic wetness index (WTI), extends the purely topography-based TWI by accounting for spatial variation in hydrologically relevant soil properties (Beven, 1986 and Beven and Kirkby 1979). The standard TI takes the form:

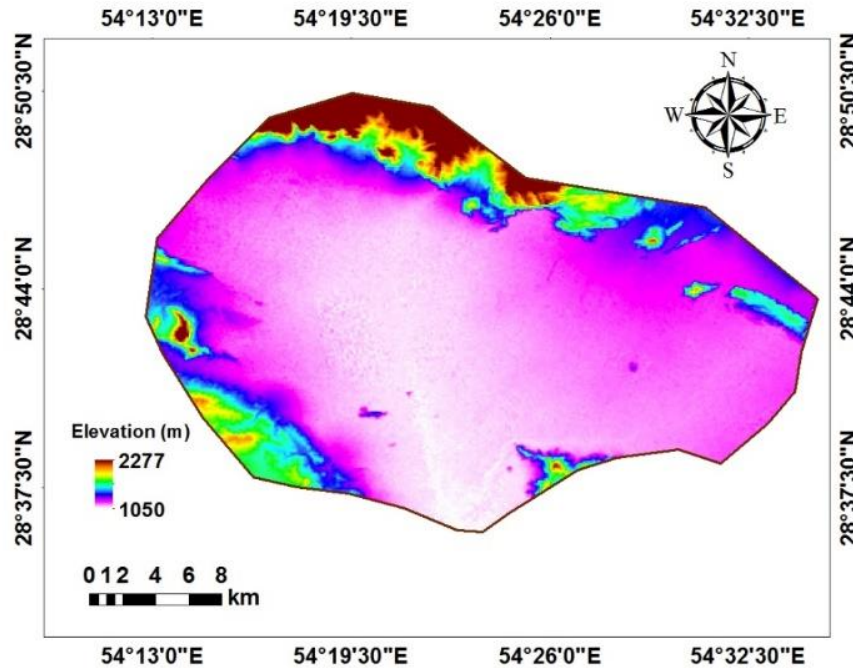
$$TWI = \ln\left(\frac{a}{\tan(\beta)}\right) \quad (5)$$

Where a is the specific catchment area [$a=A/L$, catchment area (A) divided by contour length (L)] and $\tan B$ is the slope.

The TWI index characterizes the impact parameters of slope on the hydrological processes. In terms of a specific watershed, TWI explains the water trend accumulating at a given point and the local slope indicates the effect of gravitational forces on water movement (Pourali et al., 2014). The base form is known as the steady-state TWI, which has various limitations. Many authors have modified the base form of the TWI (Eq. 5). Yong et al. (2012), Qin et al. (2011), Kopecký and Cížková, (2010), and Hjerdt et al. (2004) proposed improvements (discussed below) and Sørensen et al. (2006), Kopecký and Cížková, (2010), Ma et al. (2010), Ruhoff et al. (2011), Lewis and Holden (2012), Pei et al. (2010), Nguyen and Wilson (2010), Grabs et al. (2009) and Pourali et al. (2014) tested different flow path determination algorithms to realize the effect of a chosen method on the resultant TWI model.

2.4. Study Area

The study area has an area of about 630 km² and is located at longitude of N 28° 36' to 28° 50' and latitude of E 54° 12' to 54° 34'. Figure 4 shows a Shuttle Radar Topography Mission (SRTM) DEM data of the study area. The altitude of the study area ranges from the lowest of 1,050 m to the highest of 2,277 m. The Major study area products are wheat, citrus, cotton, maize and palm. Average of yearly rainfall in the study area is 300 mm. The study area has warm days in summer with 38-46°C and moderate winters (15-25°C) (Oryan and Sadeghi, 1997; Rezaei and Shakoor, 2011; Moein et al., 2015).



Source: <http://earthexplorer.usgs.gov>

Figure 4: Location of the study area (digital elevation model (DEM) with spatial resolution of 90 m).

3. ANALYSIS

In this study, in order to investigate the increasing of spatial resolution of DEM 90m., the attraction model was used. Also, for founding the best model and for increasing spatial resolution, three scales (2, 3, 4) with two neighborhood methods of touching and quadrant have been used. So, this can result that the increase of the scale case leads to the increase of the spatial resolution. As Figure 5 shows, with an increase in the value of scale factor, the number of sub-pixels were increased.

Also, the neighborhood of touching (T1) showed a better result than quadrant (T2) method, as the sum of the RMSE values for the touching method is lower than quadrant method. There is also a change in RMSE value of two DEMs which for DEM 90m it is around 0.32 m (6.0-6.39) which shows a slight improvement is the accuracy of DEMs with a better spatial resolution. After the production of output images for each neighborhood method, there are 3 scale factors of 2, 3 and 4. Each image is compared with ground station points using RMSE and the results then are compared.

To make a quantitative evaluation of the generated DEMs with touching and Quadrant neighborhood methods, 148 points were selected from the ground station (Points are measured by National Cartographic Center of Iran (NCC)) (Figure 5). The Root Mean Square Error (RMSE) for these points in each method for DEM 90 was calculated and is presented in Table 1. The accuracy measures for two methods are shown in Figure 6. DEM 90m generation with touching and Quadrant neighborhood for different scale factors (2, 3 and 4) are shown in Tables 2, the lowest RMSE value showed the best accuracy for increasing spatial resolution.

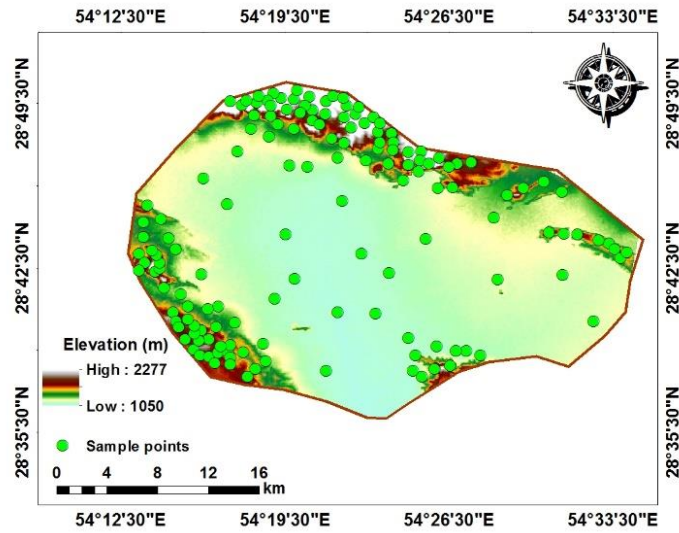


Figure 5: The location of ground sample points by National Cartographic Center of Iran (NCC).

Table 1: Output DEMs RMSE values (S=Scale factor, T1=Touching method, T2=Quadrant method).

DEM	RMSE
S=2, T1	6.06
S=3, T1	8.09
S=4, T1	7.76
S=2, T2	6.06
S=3, T2	8.23
S=4, T2	8.89

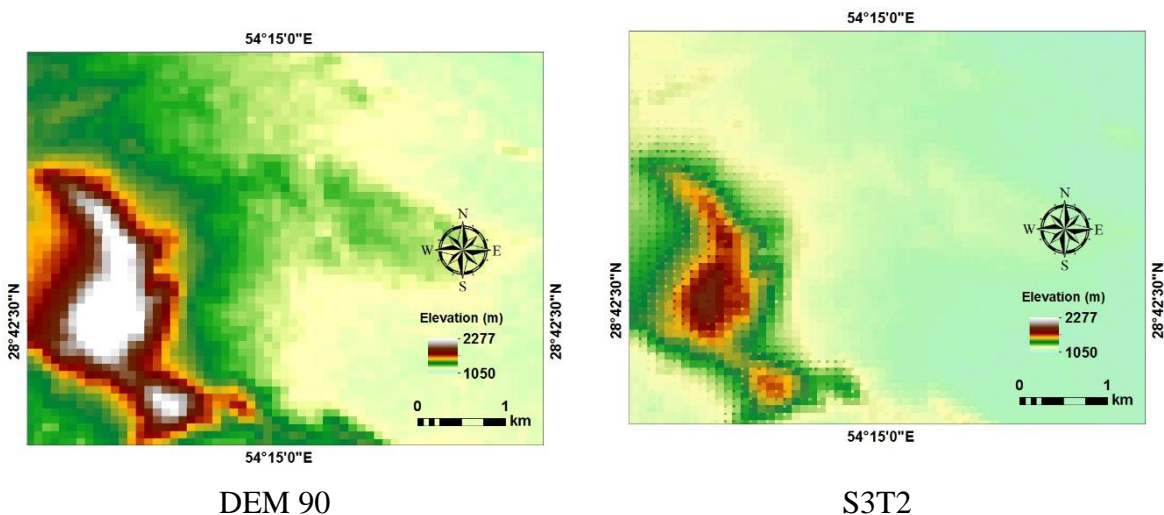


Figure 6: DEMs generated using touching and Quadrant neighborhood with different scale factors.

As the empirical perspective increases in scale factor, the accuracy of models decreases and it is because of the way that the sub-pixel model gathers information from surrounding pixels. Because each sub-pixel should get a value from surroundings so when the scale factor increases the number of sub-pixels in a pixel increases and then the way to set a value to each sub-pixel faces some inaccuracy. For example Figure 2 with different scale factors in Quadrant method

when scale factor increases to find value of sub-pixel in position of (1,1) three of surrounding pixels are used but to calculate value of sub-pixel (2,3) in scale factor 2, all five surrounding pixels are used and because here only one class (only elevation) is used so the information in lower scale factors is more accurate than higher ones. In general, here with an increase of resolution because sub-pixel values are divided spatially and then recalculated it makes them more accurate when we use ground station points to calculate RMSE but when scale factor increases to more than 2 the accuracy in sub-pixels starts to decrease.

After the determination of the best model for extracting TWI was prepared it was used in GIS software for the study area (Figure 7).

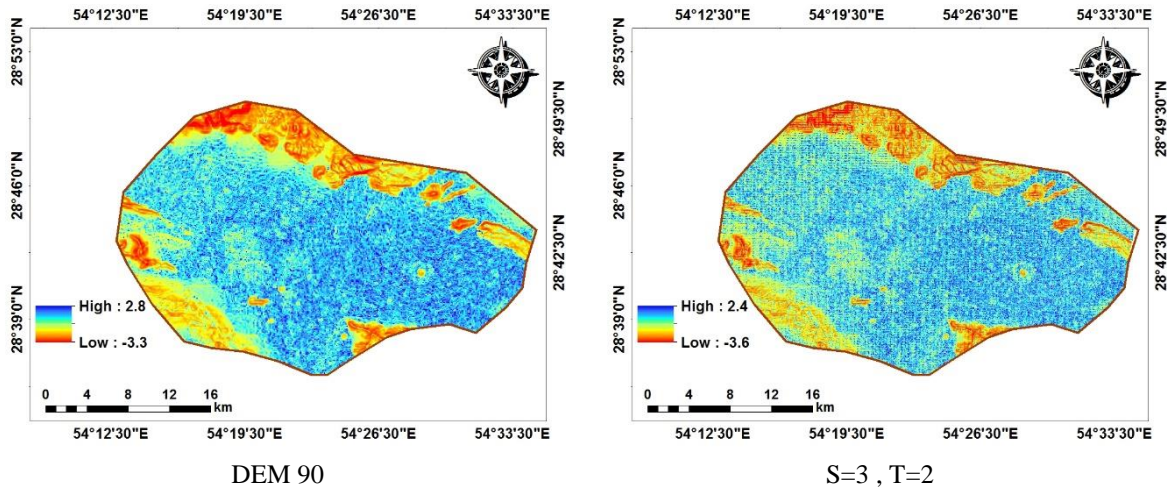


Figure 7: TWI map using attraction model (right) and DEM 90m (left).

According to Figure 7, it was determined that TWI using attraction model (S=3, T=2) has more details than TWI extraction from DEM 90m. According to the results, it was determined that the attraction model algorithm has a few simple basic rules. The assignment of pixels is performed during a one-step process, always yielding the same output, resulting in another advantage: the absence of iterations. There is no need for calibration/training as is the case with machine learning methods. This limits computation time, resulting in a relatively fast algorithm (less than 3 minutes with scale factor 2 for a 3601*3601-pixel image on an Intel core I 7+, 1.60 GHz processor).

Another advantage is its ability to deal with soft classifications with more than two classes, as there are 8 neighboring's around each pixel this algorithm can deal with maximum 8 different classes. An extensive comparison of different sub-pixel mapping algorithms is the subject of another research. The sub-pixel attraction model was used by many researches, for increasing the spatial resolution of land cover, land use and satellite image that all showed using the methods of increasing the spatial resolution can lead to archive the image with high spatial resolution and high information of region area (Schneider, 1993; Foody, 1998; Aplin and Atkinson, 2001; Verhoeve and De Wulf, 2002; Mertens et al. 2014). Mertens et al. (2014) used them in satellite image. The algorithm was evaluated both visually and quantitatively using RMSE accuracy index.

The resulting images showed increased accuracy when using a scale factor of 2 and slightly decrease in accuracy in higher scale factors. Using sub-pixel methods, we can achieve more accuracy in some cases. It also shows that we can apply these methods on Aster DEM and the output of 15m DEMs could be used with acceptable accuracy.

4. CONCLUSIONS

In this paper, prepared TWI from different spatial resolutions of DEMs was performed for attraction model and DEM 90m. Based on the results obtained, it was determined that the attraction model (S3, T2) produced higher accuracy than DEM 90m for extraction rivers. In fact the algorithm was evaluated both visually and quantitatively using RMSE accuracy index. The basic assumption is the spatial dependence as adopted by Mertens et al. (2014).

However, spatial dependence in this study is acting across different scale levels resulting in a sub-pixel interaction. The results showed that using the method the spatial resolution of DEM with lower time and cost, could be increased. To sum up using sub-pixel model both the accuracy and spatial resolution of input DEMs are increased and it gives more opportunity to use higher resolution DEMs in the study of environment models.

ACKNOWLEDGEMENTS

The authors would like to acknowledge Shiraz University, the Department of Range and Watershed Management and also Organization National Cartographic Center of Iran (NCC) for providing the point dataset and their general assistance in this study.

REFERENCES

- Altaf, F., Meraj, G., and Romshoo, S.A. 2013. Morphometric Analysis to Infer Hydrological Behaviour of Lidder Watershed, Western Himalaya, India. Hindawi Publishing Corporation. *Geography Journal*. Volume 2013, Article ID 178021, 14 pages.
- Beven, K., and Kirkby, M. 1979. A physically based, variable contributing area model of basin hydrology/Un modèle à base physique de zone d'appel variable de l'hydrologie du bassin versant. *Hydrological Sciences Journal*, 24(1), 43–69.
- Buffington, J.M., Montgomery, D.R. 2013. Geomorphic classification of rivers. In: Shroder, J. (Editor in Chief), Wohl, E. (Ed.), *Treatise on Geomorphology*. Academic Press, San Diego, CA, vol. 9, Fluvial Geomorphology, pp. 730–767.
- Chorley, R.J. and Kennedy, B.A. (Eds.), 1971, *Physical Geography, A systematic approach*, p 370 (London, Prentice Hall).
- Christofolletti, A. and Oka-Fiori, C., 1980, O uso da densidade de rios como element para caracterizar as farmacoes superficiais, *Not. Geomorfol*, 20 (39&40), pp. 73-85.
- Deen, M., 1982, *Geomorphology and Land use: A Case Study of Mewat, thesis submitted to the center for the study of regional development*, JNU, New Delhi.
- Zavadil, E.A., Stewardson, M.J., Turner, M.E., Ladson, A.R. 2012. An evaluation of surface flow types as a rapid measure of channel morphology for the geomorphic component of river condition assessments. *Geomorphology*, Volumes 139–140, 15 February 2012, Pages 303-312.
- Farr, T.G., Rosen, P.A., Caro, E., Crippen, R., Duren, R., Hensley, S., Kobrick, M., Paller, M., Rodriguez, E., Roth, L., Seal, D., Shaffer, S., Shimada, J., Umland, J., Werner, M., Oskin, M., Burbank, D., and Alsdorf, D. 2007. The Shuttle Radar Topography Mission. *Rev. Geophys.*45, RG2004, doi: 10.1029/2005RG000183.

- Gardiner, V. 1982. Drainage basin morphometry: quantitative analysis of drainage basin form. In *Perspectives in Geomorphology*, H.S. Sharma (Ed.), pp. 107-142 (New Delhi, Concept Publishing Company).
- Grabs, T., Seibert, J., Bishop, K., and Laudon, H. 2009. Modeling spatial patterns of saturated areas: a comparison of the topographic wetness index and a dynamic distributed model. *Journal of Hydrology*, 373(1), 15–23.
- Gupta, H.K., Rao, V.D. and Singh, J., 1982. Continental collision tectonics: Evidence from the Himalaya and the neighbouring regions. *Tectonophysics*, 81, pp. 213-238.
- Hjerdt, K., McDonnell, J., Seibert, J., and Rodhe, A. 2004. A new topographic index to quantify downslope controls on local drainage. *Water Resources Research*, 40(5), W05602.v
- Banasik, K., and Hejduk, A. 2015. Ratio of basin lag times for runoff and sediment yield processes recorded in various environments. *Sediment Dynamics from the Summit to the Sea* (Proceedings of a symposium held in New Orleans, Louisiana, USA, 11–14.
- Kopecký, M., and Cížková, Š. 2010. Using topographic wetness index in vegetation ecology: does the algorithm matter? *Applied Vegetation Science*, 13(4), 450–459.
- Lewis, G., and Holden, N.M. 2012. A comparison of grid-based computation methods of topographic wetness index derived from digital elevation model data. *Biosystems Engineering Research Review*, 17, 103.
- Opekunova, M.Y. 2014. Channel deformations and geomorphological processes in the upper reach of the Lena River. *Geography and Natural Resources* . Volume 35, Issue 2, pp 157-164.
- Ma, J., Lin, G., Chen, J., and Yang, L. 2010. June. An improved topographic wetness index considering topographic position. In 2010 18th International Conference on Geoinformatics (pp. 1-4). IEEE.
- LeBlanc, M., and Favreau, G. 2006. Reconstruction of Megalake Chad using Shuttle Radar Topographic Mission data. *Palaeogeography, Palaeoclimatology, Palaeoecology*, 12, pp. 213-216. [9] HEIM, A. and GANSSER, A., 1939, Central Himalaya; geological observations of the Swiss expedition 1936. *Schweizer. Naturf. Ges., Denksch.* 73 (1), p. 245.
- Meei Ling, L., and Kuo Lung, W., 2005. Assessment of Landslides Caused by Earthquake- Case Study of Chi-Chi Earthquake in Taiwan, 1999. *Geophysical Research Abstracts*, 7: 08654.
- Melton, M.A., 1957. An Analysis of the Relations among the Elements of Climate, Surface Properties and Geomorphology, In: *Technical Report 11*, New York Department of Geology, Columbia University.
- Moein, M., Zarshenas, M.M., Khademian, S., Razavi, A.D. 2015. Ethnopharmacological review of plants traditionally used in Darab (south of Iran). *Trends in Pharmaceutical Sciences* 2015; 1(1): 39-4.
- Mokarram, M., and Sathyamoorthy, D. 2015. Morphometric analysis of hydrological behavior of north fars watershed, Iran. *European Journal of Geography*, 6(4), 88-106.

- Morariu, T., Pisota, I. and Buta, I., 1962. General hydrology, (Bucharest: Ed. Didactica si pedagogica), (in Romanian).
- Morisawa, M.F., 1968, *Streams their Dynamics and Morphology*, pp. 153 – 154 (New York: McGraw Hill).
- Naithani, N.P. and Rawat, G.S., 1990, Morphometric Analysis of Bhagirathi Valley between Maneri and Gangnani area, district Uttarkashi, Garhwal Himalaya. In *Ecology of the Mountain Waters*, SD Bhatt and RK Pande (Eds.), pp. 33-40 (New Delhi: Ashish Publishing House).
- Nayar, V., Natarajan, K. 2013. Quantitative Morphometric analysis of Kosasthalaiyar sub basin (Chennai basin) using remote sensing (SRTM) data and GIS techniques. *International journal of geomatics and geosciences*. Volume 4, No 1.
- Nguyen, T. T. M., and Wilson, J. P. 2010. Sensitivity of quasi-dynamic topographic wetness index to choice of DEM resolution, flow routing algorithm, and soil variability.
- Oryan A, Sadeghi M. An epizootic of besnoitiosis in goats in Fars province of Iran. *Veterinary Research Communications*, 1997, 21:559-70.
- Parveen1, R., Kumar, U., Kumar Singh V. 2012. Geomorphometric Characterization of Upper South Koel Basin, Jharkhand: A Remote Sensing & GIS Approach. *Journal of Water Resource and Protection*, 2012, 4, 1042-1050.
- Pei, T., Qin, C. Z., Zhu, A., Yang, L., Luo, M., Li, B., et al. 2010. Mapping soil organic matter using the topographic wetness index: a comparative study based on different flow-direction algorithms and kriging methods. *Ecological Indicators*, 10(3), 610–619.
- Pidwirny, M. 2006. "Erosion and Deposition". Fundamentals of Physical Geography, 2nd Edition. Date Viewed. <http://www.physicalgeography.net/fundamentals/10w.html>
- Qin, C.Z., Zhu, A.X., Pei, T., Li, B.L., Scholten, T., Behrens, T. et al. 2011. An approach to computing topographic wetness index based on maximum downslope gradient. *Precision Agriculture*, 12(1), 32–43.
- Rezaei, M.R., and Shakoor, A. 2011. Study of Some Concerned Factors among Rural Farmers of Darab City (Fars Province of Iran) Based on Economical Geography View. *Development*. 3:4.
- Ruhoff, A. L., Castro, N. M. R., and Risso, A. 2011. Numerical modelling of the topographic wetness index: an analysis at different scales. *International Journal of Geosciences*, 2(4), 476–483.
- Pourali, S.H., Arrowsmith, C., Chrisman, N., Matkan, A.A., and Mitchell, D. 2014. Topography Wetness Index Application in Flood-Risk-Based Land Use Planning. *Appl. Spatial Analysis* DOI 10.1007/s12061-014-9130-2.
- Shrimali, S.S., Aggarwal, S. P. and Samra, J. S. 2001. Prioritizing erosionprone areas in hills using remote sensing and GIS – a case study of the Sukhna Lake catchment, Northern India, *International Journal of Applied Earth Observation and Geoinformation*, 3(1), pp 5460.
- Singh, S. (Ed.), 2000, *Geomorphology*, (Allahabad: Prayag Pustak Bhawan), p 642.

- Singh, S., 1972, Altimetric analysis, A morphometric technique of land form study, National Geographer, Vol. VII, Allahabad.
- Sörensen, R., Zinko, U., and Seibert, J. 2006. On the calculation of the topographic wetness index: evaluation of different methods based on field observations. *Hydrology and Earth System Sciences Discussions*, 10(1), 101–112.
- Bolch, T., 2004. Using ASTER and SRTM DEMS for Studying Glaciers and Rock glaciers in Northern Tien Shan. In: Proceedings Part I of the Conference “Theoretical and applied problems of geography on a boundary of centuries”, 8-9 June 2004, Almaty, Kasakhstan, pp. 254- 258.
- Bolch, T., Kamp, U., and Olsenholler, J. 2005. Using ASTER and SRTM DEMs for studying geomorphology and glaciation in high mountain areas. In: *New Strategies for European Remote Sensing*, Olui (ed.) (Rotterdam: Millpress).
- Wang, Y., Liao, M., Sun, G. and Gong, J., 2005, Analysis of the water volume, length, total area and inundated area of the Three Gorges Reservoir, China using the SRTM DEM data. *International Journal of Remote Sensing*. 26 (18), pp. 4001–4012.
- Werner M. 2001. Shuttle Radar Topography Mission. Mission overview. *Journal of Telecommunication* 55, 75-79.
- Yildiz, O., 2004, An investigation of the effect of drainage density on hydrologic response, *Turkish Journal of Engineering and Environmental Sciences*, 28, pp. 85-94.
- Yong, B., Ren, L. L., Hong, Y., Gourley, J. J., Chen, X., Zhang, Y. J., et al. (2012). A novel multiple flow direction algorithm for computing the topographic wetness index. *Hydrology Research*, 43(1–2), 135–145.
- Zavoianu, I., 1985, Morphometry of drainage watershed, *Developments in Water Science* 20, pages 251 (Bucharest: Editura Academiei).